Comparison of Radiation Pressure Perturbations on Rocket Bodies and Debris at Geosynchronous Earth Orbit

Charles J. Wetterer and Keric Hill
Integrity Applications Incorporated - Pacific Defense Solutions
Moriba Jah
Air Force Research Laboratory

CONFERENCE PAPER

Recent research has highlighted the need for physically consistent radiation pressure and Bidirectional Reflectance Distribution Function (BRDF) models. This paper seeks to evaluate the impact of BRDF-consistent radiation pressure models compared to changes in the other BRDF parameters. The differences in orbital position arising because of changes in the shape, attitude, angular rates, BRDF parameters, and radiation pressure model are plotted as a function of time for simulated rocket bodies and debris at geosynchronous orbit (GEO). The initial position and velocity of the space object is kept fixed, and the orbital position difference between a baseline orbit and the perturbed orbit are plotted as a function of time. This is similar to how the effects of perturbations have been visualized in the past in commonly used astrodynamics references.

1. INTRODUCTION

There are many sources of perturbations when propagating an orbit forward in time including non-spherical gravitational effects, third-body effects, and radiation pressure. Solar radiation pressure (SRP) depends on both the space object (SO)'s attitude and the surface properties as expressed by the BRDF. Wetterer et al.[1] first demonstrated how the SRP acceleration should be physically consistent with the associated BRDFs to achieve high-precision orbit propagation.

The work presented here seeks to compare the magnitude of the perturbations caused by using a simplified SRP acceleration model as compared to the physically-consistent SRP model with those resulting from changes in other parameters associated with the SRP. The initial position and velocity of the space object is kept fixed, and the orbital position difference between a baseline orbit and the perturbed orbit are plotted as a function of time. This is similar to how the effects of perturbations have been visualized in the past in commonly used astrodynamics references[2]. First, the shape model, BRDF model, and the SRP model are described. Finally, the simulation setup and results are presented.

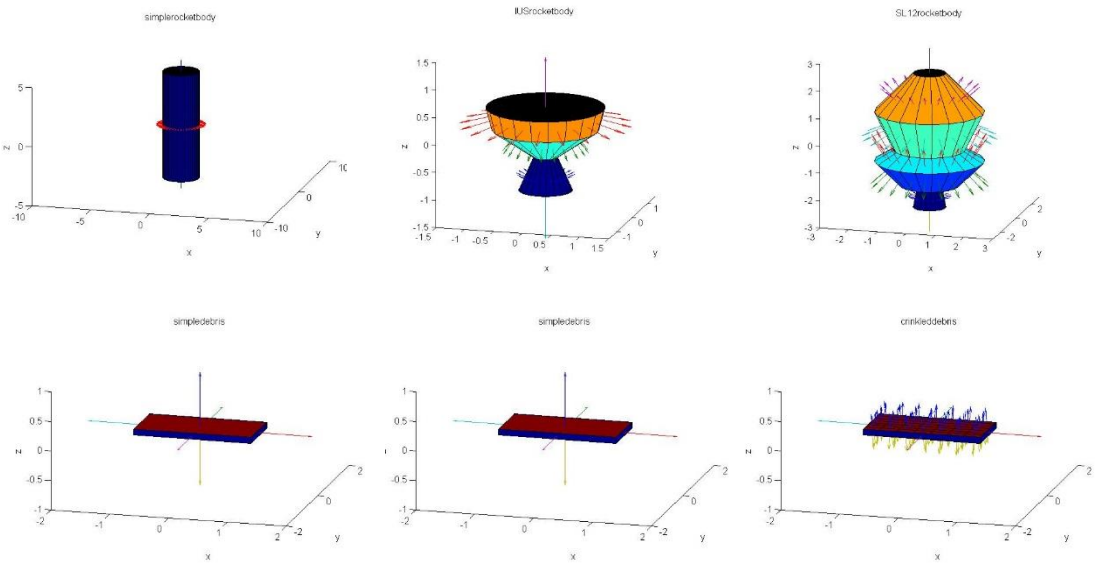

Figure 1. Shape Models

Report Documentation Page

Form Approved
OMB No. 0704-0188

1. REPORT DATE	2. REPORT TYPE	3. DATES COVERED
SEP 2014		**00-00-2014 to 00-00-2014**

4. TITLE AND SUBTITLE	5a. CONTRACT NUMBER
Comparison of Radiation Pressure Perturbations on Rocket Bodies and Debris at Geosynchronous Earth Orbit	5b. GRANT NUMBER
	5c. PROGRAM ELEMENT NUMBER
6. AUTHOR(S)	5d. PROJECT NUMBER
	5e. TASK NUMBER
	5f. WORK UNIT NUMBER
7. PERFORMING ORGANIZATION NAME(S) AND ADDRESS(ES) **Integrity Applications Incorporated - Pacific Defense Solutions,535 Lipoa Parkway Ste 101,Kihei,HI,96753**	8. PERFORMING ORGANIZATION REPORT NUMBER
9. SPONSORING/MONITORING AGENCY NAME(S) AND ADDRESS(ES)	10. SPONSOR/MONITOR'S ACRONYM(S)
	11. SPONSOR/MONITOR'S REPORT NUMBER(S)

12. DISTRIBUTION/AVAILABILITY STATEMENT
Approved for public release; distribution unlimited

13. SUPPLEMENTARY NOTES
presented at the Advanced Maui Optical and Space Surveillance Technologies (AMOS) Conference, 9-12 Sep 2014, Maui, HI.

14. ABSTRACT

15. SUBJECT TERMS

16. SECURITY CLASSIFICATION OF:			17. LIMITATION OF ABSTRACT	18. NUMBER OF PAGES	19a. NAME OF RESPONSIBLE PERSON
a. REPORT	b. ABSTRACT	c. THIS PAGE			
unclassified	**unclassified**	**unclassified**	**Same as Report (SAR)**	**10**	

2. SHAPE MODEL DESCRIPTIONS

Each shape model is composed of a number of flat facets with each facet having a surface area, position, and normal direction. Six shape models are considered in this paper. Figure 1 shows a rendering of each model and Table 1 displays relevant information about each.

Table 1. Shape Model Descriptions

name	mass (kg)	description
simplerocketbody	1500	9 × 3 m (cylinder) – rough mass and dimensions of Centaur upper stage
IUSrocketbody	300	1.5 × 2.0 m (truncated cones) – rough mass and dimensions of Inertial Upper Stage (IUS)'s stage II and spacecraft interface
SL12rocketbody	2400	4.9 × 3.7 m (truncated cones) – rough mass and dimensions of Blok DM SL-12 upper stage
simpledebris(1)	1	2 × 1 × 0.1 m (rectangular prism)
simpledebris(2)	5	2 × 1 × 0.1 m (rectangular prism)
crinckleddebris	5	2 × 1 × 0.1 m (rectangular prism with 49 facet on ± z-faces with 1° random spread of normal vectors)

3. BIDIRECTIONAL REFLECTANCE DISTRIBUTION FUNCTION MODEL

Each surface on the shape model may represent a different material, and each material that makes up the model could reflect light differently. Thus, a model might have many parameters that specify its surface properties. The function that defines how light is reflected from an opaque surface with a given surface normal direction ($\hat{\mathbf{N}}$), illumination direction ($\hat{\mathbf{L}}$ with angles θ_i and ϕ_i from $\hat{\mathbf{N}}$), and observer direction ($\hat{\mathbf{V}}$ with angles θ_r and ϕ_r from $\hat{\mathbf{N}}$) as shown in Fig. 2 is called the bidirectional reflectance distribution function (BRDF).

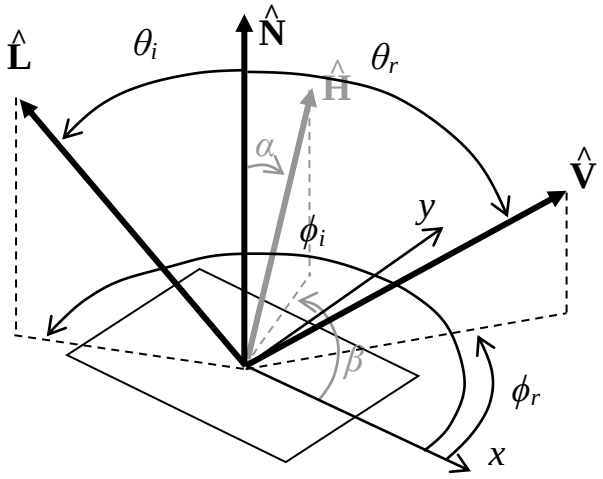

Figure 2. The Geometry of Reflection

The BRDF is given by

$$f_r(\theta_i,\phi_i;\theta_r,\phi_r;\lambda)=\frac{dL_r(\theta_r,\phi_r;\lambda)}{dE_i(\theta_i,\phi_i;\lambda)} \tag{1}$$

where dL_r is the reflected radiance in $\mathrm{Wm^{-2}sr^{-1}}$ and dE_i is the irradiance in $\mathrm{Wm^{-2}}$. The bisector vector between the illumination source and the observer is

$$\hat{\mathbf{H}}=\left(\hat{\mathbf{L}}+\hat{\mathbf{V}}\right)\Big/\left|\hat{\mathbf{L}}+\hat{\mathbf{V}}\right| \tag{2}$$

with angles α and β from $\hat{\mathbf{N}}$ and is used in many analytic BRDF models.

There are many different reflectance models that could be used, but all can be expressed in a common nomenclature with the general BRDF calculated by

$$f_r = \left(dR_d + sR_s\right) \tag{3}$$

which depends on the diffuse bidirectional reflectance (R_d) and the specular bidirectional reflectance (R_s) and the fraction of each to the total (d and s respectively where $d + s = 1$). These bidirectional reflectances are calculated differently for the various models. In this paper we will use the Ashikhmin-Shirley BRDF[3], also known as the Anisotropic Phong BRDF, where the diffuse and specular bidirectional reflectances are calculated using

$$R_d = \frac{28\rho}{23\pi}\left(1 - sF_0\right)\left(1 - \left(1 - \frac{\hat{\mathbf{N}}\cdot\hat{\mathbf{L}}}{2}\right)^5\right)\left(1 - \left(1 - \frac{\hat{\mathbf{N}}\cdot\hat{\mathbf{V}}}{2}\right)^5\right) \tag{4}$$

$$R_s = \frac{\sqrt{\left(n_u + 1\right)\left(n_v + 1\right)}}{8\pi}\frac{F}{\left(\hat{\mathbf{V}}\cdot\hat{\mathbf{H}}\right)\max\left[\hat{\mathbf{N}}\cdot\hat{\mathbf{L}}, \hat{\mathbf{N}}\cdot\hat{\mathbf{V}}\right]}\left(\cos\alpha\right)^{n_u\cos^2\beta + n_v\sin^2\beta} \tag{5}$$

where (4) is a non-Lambertian diffuse BRDF, and the Fresnel reflectance (F) in (5) is given by Schlick's approximation[4]

$$F = F_0 + \left(\frac{1}{s} - F_0\right)\left(1 - \hat{\mathbf{V}}\cdot\hat{\mathbf{H}}\right)^5 \tag{6}$$

In addition to d, ρ and F_0, the Ashikhmin-Shirley BRDF has two exponential factors (n_u, n_v) that define the anisotropic reflectance properties of each surface. Without loss of functionality, the diffuse reflectance and the specular reflectance at normal incidence can be set equal to each other ($\rho = F_0$) and the difference between the diffuse and specular reflectances displayed in the diffuse fraction parameter, d. Additionally, for the sake of simplicity, in this paper the two exponential factors are set equal to each other as well ($n_u = n_v = n$). Thus, there are three unique surface parameters per surface (n, ρ, d). These surface parameters have constraints ($n > 0$, $0 \le \rho \le 1$, $0 \le d \le 1$). A final assumption is that every facet on the shape model is represented by the same BRDF parameters. In the simulations of the next section, the reflectance parameter is set to $\rho = F_0 = 0.1$, 0.5, and 0.9 representing low reflectivity, mid reflectivity, and high reflectivity, the diffuse fraction parameter is set to $d = 0.2$ and 0.8 representing a highly specular and a highly diffuse surface, and the exponential factor parameter is set to $n_u = n_v = n = 50$ and 500 representing a "dull" and "sharp" specular peak.

The curved cylindrical surface of *simplerocketbody* is modeled with 50 flat facets. The curved truncated conic sections of *IUSrocketbody* and *SL12rocketbody* are modeled with 20 flat facets. To produce accurate light curves of curved surfaces, however, requires a larger number of facets depending on the BRDF exponential factor of the surface. This is discussed further in the appendix.

4. SOLAR RADIATION PRESSURE (SRP) MODEL

The acceleration caused by the SRP can be calculated by summing the individual contributions of all the constituent illuminated "facets" that make up the object. The acceleration is

$$\mathbf{a}_{SRP} = -\sum_{k=1}^{N_{facets}}\int_0^\infty \frac{F_i(\lambda)A_k f_k\left(\hat{\mathbf{L}}\cdot\hat{\mathbf{N}}_k\right)_+}{m_{so}c}\left(\hat{\mathbf{L}} + \left(\int_0^{2\pi}\int_0^{\pi/2} f_r\cos\theta_r\hat{\mathbf{V}}d\theta_r d\phi_r\right)_k\right)d\lambda \tag{7}$$

where $F_i(\lambda)$ is the solar flux (in $\mathrm{Wm^{-2}nm^{-1}}$), A_k is the facet area, f_k is the fraction of the facet that is illuminated (due to self-shadowing), m_{so} is the mass of the object, c is the speed of light, and the BRDF for each facet is integrated over all observer directions and all wavelengths. Additionally, $(x)_+ = xH(x)$ where $H(x)$ is the Heaviside step function which is unity for positive values and zero elsewhere.

For certain BRDFs, the integral can be solved analytically. For example, the BRDF with a Lambertian diffuse component and purely "mirror-like" specular component (where $\hat{\mathbf{R}} = 2\left(\hat{\mathbf{L}} \cdot \hat{\mathbf{N}}\right)\hat{\mathbf{N}} - \hat{\mathbf{L}}$ is the direction of mirror-like reflection of $\hat{\mathbf{L}}$) is given by

$$f_r = d\left(\frac{\rho}{\pi}\right) + s\left(\frac{F_0 \delta\left(\hat{\mathbf{V}} - \hat{\mathbf{R}}\right)}{\cos\theta_i}\right) \tag{8}$$

where δ is the Delta function, yields an acceleration due to the SRP of

$$\mathbf{a}_{SRP} = -\sum_{k=1}^{N_{facets}} \frac{F_{sun} A_k f_k \left(\hat{\mathbf{L}} \cdot \hat{\mathbf{N}}_k\right)_+}{m_{SO} c} \left(\left(1 - s_k \left(F_0\right)_k\right)\hat{\mathbf{L}} + \left(\frac{2}{3} d_k \rho_k + 2 s_k \left(F_0\right)_k \hat{\mathbf{L}} \cdot \hat{\mathbf{N}}_k \right)\hat{\mathbf{N}}_k \right) \tag{9}$$

where F_{sun} is the total solar flux over all wavelengths. This is the conventional formula typically used to calculate the SRP acceleration for a facet-based model (e.g. equivalent to equations derived in Appendix A in Ref. [5]).

For a more complicated BRDF, such as the Ashikhmin-Shirley model described previously, the exact solution obtained by numerically integrating Eq. (7) is different than the idealized solution obtained by Eq. (9). Ref. [1] developed a way of computing correction factors for Eq. (9) and the acceleration is calculated by using

$$\mathbf{a}_{SRP} = -\sum_{k=1}^{N_{facets}} \frac{F_{sun} A_k f_k \left(\hat{\mathbf{L}} \cdot \hat{\mathbf{N}}_k\right)_+}{m_{SO} c} \left(\begin{array}{l} \left(1 - \left(\Delta_{s1}\right)_k s_k \left(F_0\right)_k\right)\hat{\mathbf{L}} \\ + \left(\frac{2}{3} \left(\Delta_d\right)_k d_k \rho_k + 2 \left(\Delta_{s2}\right)_k s_k \left(F_0\right)_k \hat{\mathbf{L}} \cdot \hat{\mathbf{N}}_k \right)\hat{\mathbf{N}}_k \end{array} \right) \tag{10}$$

where the Δ factors depend on the illumination angle and parameters within the BRDF model. Thus, for $\Delta_d = 1$, the diffuse reflectance is Lambertian and for $\Delta_{s1} = \Delta_{s2} = 1$, the specular reflectance is mirror-like. The further these Δ factors are from unity, the greater the difference between the BRDF model and the idealized BRDF of Eq. (9).

The SRP acceleration is highly dependent on the object's attitude. For the rocket body models, it is assumed they are single axis rotators about the model's x-axis and have one of three initial attitudes (corresponding to the rotation axis in the x, y, and z ECI directions) and one of two initial angular rates (corresponding to a "slow" rotation with a period of about 1 hour and a "fast" rotation with a period of about 5 minutes). For the debris models, the same initial attitude is chosen for all cases (corresponding to body frame equal to ECI frame) and one of four initial angular rates (corresponding to two different "slow" tumbles and two different "fast" tumbles where "slow" and "fast" are comparable to the rocket body angular rates). For all cases, the SRP model of Eq. (9) and Eq. (10) are also simulated.

5. SIMULATIONS SETUP AND RESULTS

The orbit was initialized to that of the two-line element (TLE) of the near geosynchronous rocket body SSN 19550 with observations simulated starting at 2013 May 01 at 0:00:00 UT and extending to 2013 Aug 01 at 0:00:00 UT (92 days). Specifically, the initial Cartesian state is r = [-41557.77598 -6572.93284 1836.98724] km and v = [0.43217 -2.94731 -0.76895] km/s corresponding to an orbit with an eccentricity of 0.001568 and inclination of 14.6755 degrees.

For the rocket body models, there are a total of 144 simulated cases for each of the three shape models. For the debris models, there are a total of 96 simulated cases for each of the three shape models. Figures 3 and 4 display the total, radial, in-track, and cross-track distances from the baseline of no SRP acceleration for all cases corresponding to *simplerocketbody* and *simpledebrismodel(1)* respectively.

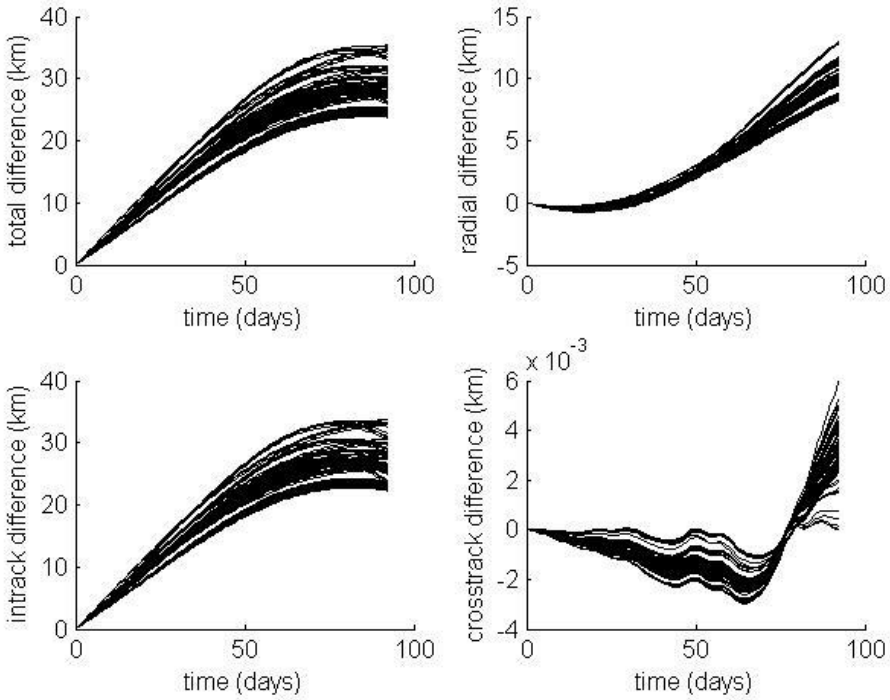

Figure 3. Orbital differences of *simplerocketbody* model from baseline

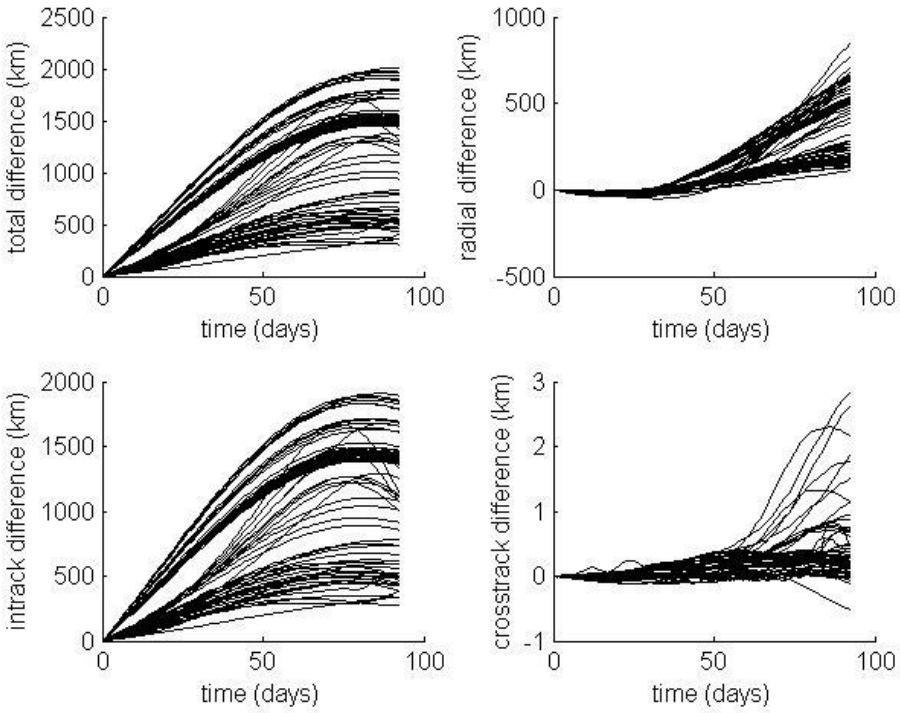

Figure 4. Orbital differences of *simpledebris(1)* model from baseline

Table 2. Simulation Results

name	AMR (max)	Average total distance (km)	Range in total distance (km)
simplerocketbody	0.0180	28.4	11.6
IUSrocketbody	0.0115	15.0	8.3
SL12rocketbody	0.0076	8.1	2.6
simpledebris(1)	2.0	1215.3	1695.4
simpledebris(2)	0.4	145.8	322.4
crinkleddebris	0.4	131.3	369.8

Table 2 lists the average total distance and spread in total distances of the full set of cases from the baseline after the 92 day propagation. In both the rocket body and debris simulations, there is a clear direct relationship between the maximum area-to-mass ratio (AMR) and both the average total distance from baseline and the range in total distances from baseline after 92 days. This is shown in Fig. 5.

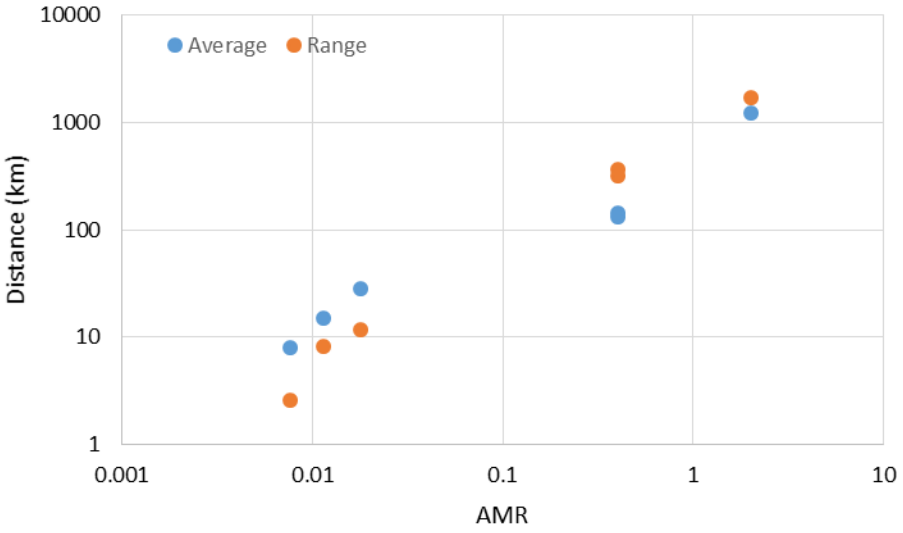

Figure 5. Average total distance and spread in total distances from baseline after 92-day propagation for the six shape models

The total difference from a baseline while varying a particular surface or environmental parameter can be calculated using all cases corresponding to each of the six shape models. For example, using the lowest value for the BRDF parameter as the baseline, Figs. 6 and 7 show the difference of the $\rho = F_0 = 0.5$ (red) cases and $\rho = F_0 = 0.9$ (green) cases from the $\rho = F_0 = 0.1$ cases where all the other parameters are the same; Figs. 8 and 9 show the difference of the $d = 0.8$ cases from the $d = 0.2$ cases where all the other parameters are the same; and Figs. 10 and 11 show the difference of the $n = 500$ cases from the $n = 50$ cases where all the other parameters are the same.

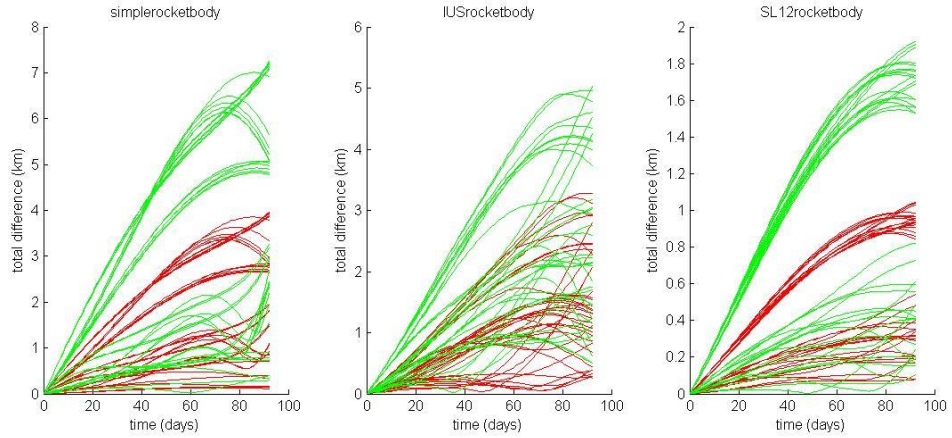

Figure 6. Orbital differences of rocket body models for BRDF reflectance parameter

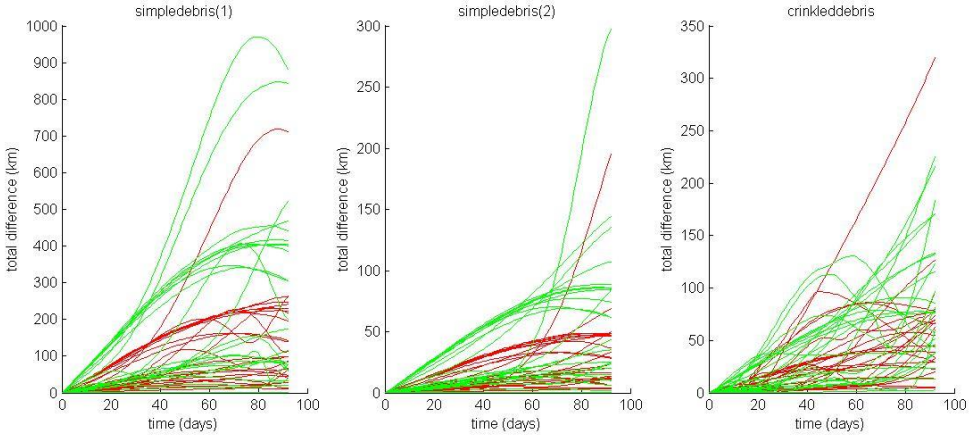

Figure 7. Orbital differences of debris models for BRDF reflectance parameter

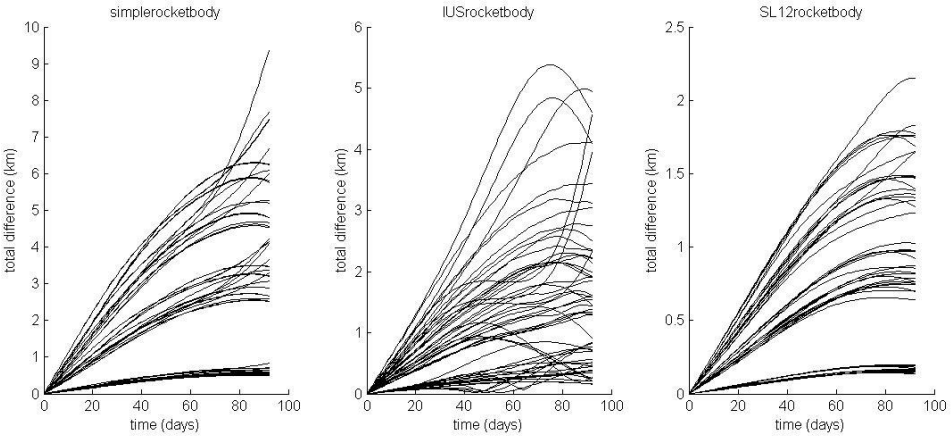

Figure 8. Orbital differences of rocket body models for BRDF diffuse fraction parameter

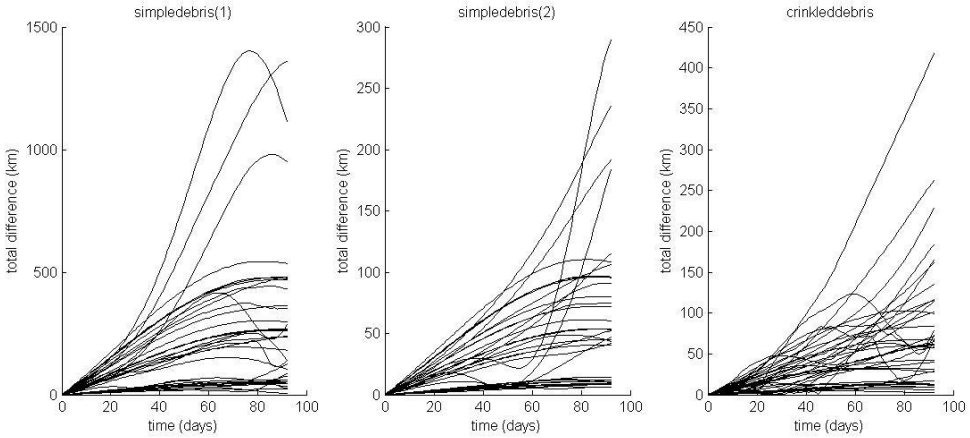

Figure 9. Orbital differences of debris models for BRDF diffuse fraction parameter

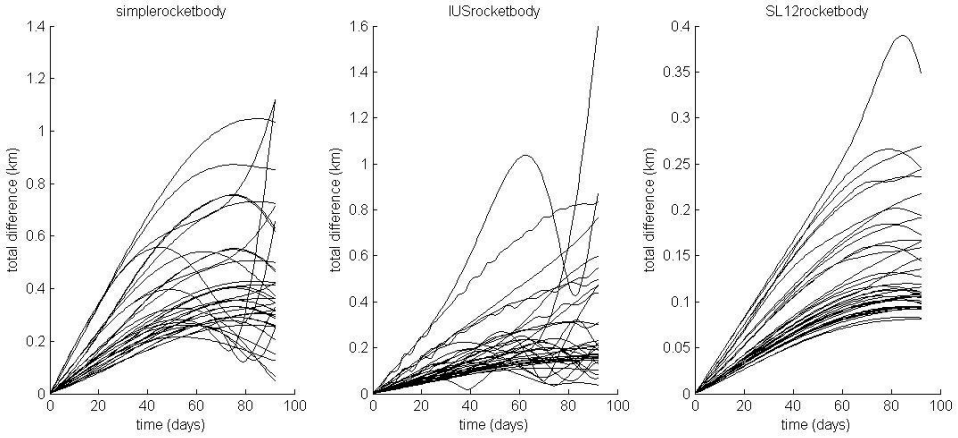

Figure 10. Orbital differences of rocket body models for BRDF exponential factor parameter

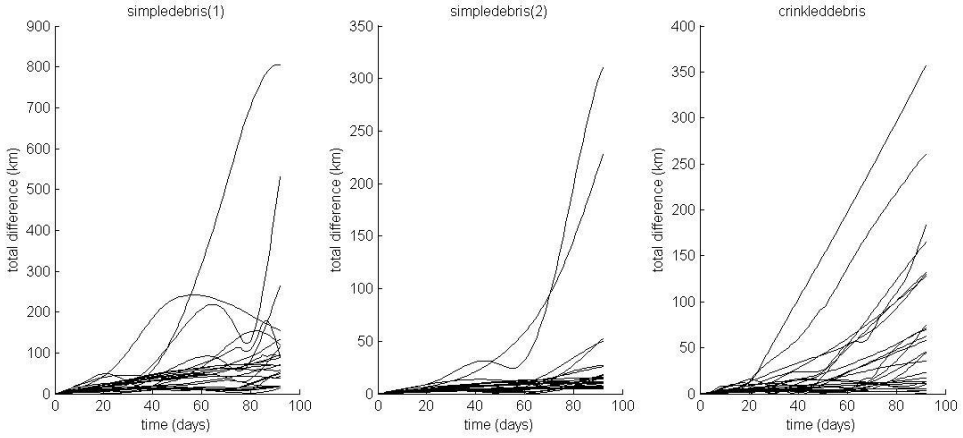

Figure 11. Orbital differences of debris models for BRDF exponential factor parameter

Figs. 12 and 13 display the total difference of the simplified SRP model from the physically-consistent SRP model with all other parameters remaining the same.

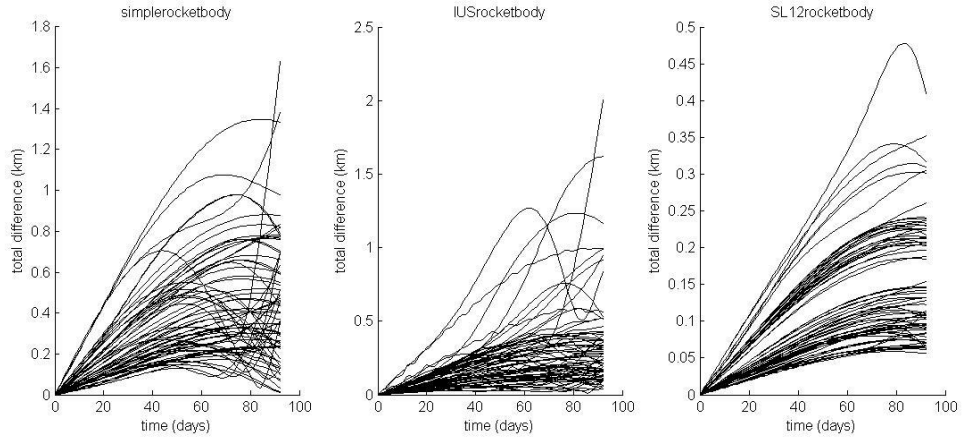

Figure 12. Orbital differences of rocket body models for SRP model used

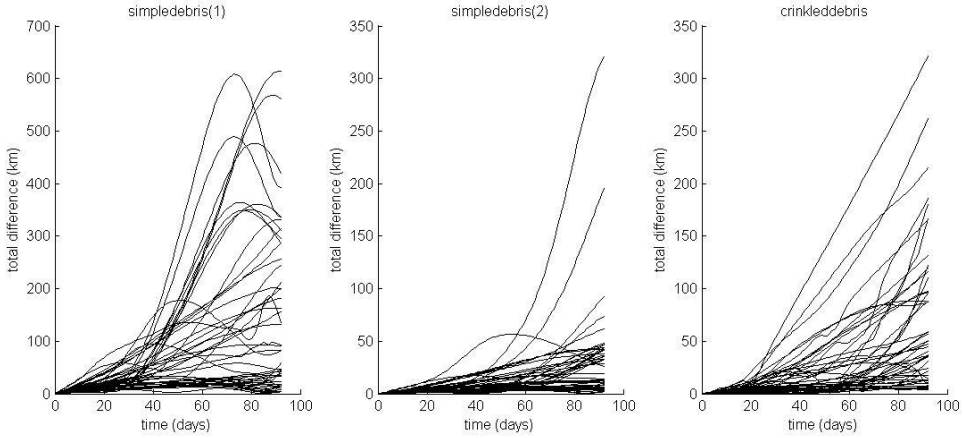

Figure 13. Orbital differences of debris models for SRP model used

The same can be done for the attitude and angular rates related cases. The difference of the initial rotation axis along the y-axis ECI cases and initial rotation axis along the z-axis ECI cases from the initial rotation axis along the x-axis ECI cases where all the other parameters are the same; the difference of the "fast" initial angular rate cases from the "slow" initial angular rate cases where all the other parameters are the same; and the difference of the two "fast" initial angular rate cases and the "slow" initial angular rate cases from the other "slow" initial angular rate cases where all the other parameters are the same. Tables 3 and 4 summarize the results by tabulating the average distance and maximum distance from baseline for each of the changing parameters and for each of the rocket body and debris models.

Table 3. Average Distance (km) from Baseline

name	ρ	d	n	Initial attitude	Initial rate	SRP model
simplerocketbody	2.98	3.39	0.22	3.62	0.23	0.46
IUSrocketbody	1.99	1.72	0.16	2.36	0.72	0.36
SL12rocketbody	0.82	0.88	0.07	0.37	0.08	0.16
simpledebris(1)	198.1	284.1	63.0	-	561.6	151.2
simpledebris(2)	45.7	64.6	18.5	-	109.3	34.3
crinkleddebris	70.9	78.5	40.0	-	115.8	71.4

Table 4. Maximum Distance (km) from Baseline

name	ρ	d	n	Initial attitude	Initial rate	SRP model
simplerocketbody	7.25	9.35	1.12	6.13	2.15	1.63
IUSrocketbody	5.03	4.95	1.59	5.83	1.90	2.01
SL12rocketbody	1.92	2.15	0.35	0.90	0.36	0.41
simpledebris(1)	880.9	1359.0	805.0	-	1346.0	613.3
simpledebris(2)	297.8	289.3	310.5	-	298.5	320.5
crinkleddebris	319.4	417.3	357.1	-	456.0	321.5

6. CONCLUSION

Whereas the choice of solar radiation pressure (SRP) model (whether physically consistent or simplified) does have a measureable effect on the perturbations of rocket body and debris objects in near-geosynchronous orbits, it is a less significant than changes in other parameters that govern the magnitude of the SRP acceleration. Namely, these parameters include those associated with the bidirectional reflectance distribution function (BRDF) (reflectance, diffuse fraction, and exponential factor) and attitude (initial attitude and angular rates). Most important of these appear to be the overall diffuse and specular reflectance and the diffuse to specular fraction. In the rocket body cases where the object started as a simple rotator, the initial attitude was also relatively significant while the exponential factor and initial angular rate along with the SRP model were less so. In the debris cases where the object started in a tumbling state (and initial attitude was not changed), the initial angular rates appeared to also be relatively significant while only the exponential factor and SRP model were less so.

ACKNOWLEDGEMENTS

This work is sponsored by a Small Business Innovative Research (SBIR) contract FA9453-11-C-0154 by the Air Force Research Laboratory (AFRL) at Kirtland Air Force Base. The authors also wish to acknowledge useful discussions and technical contributions made by other members of the SBIR team: John Crassidis, Rich Linares, and Paul Cefola of University at Buffalo, and C. Channing Chow of Pacific Defense Solutions, LLC

REFERENCES

[1] Wetterer, C. J., Linares, R., Crassidis, J. L., Kelecy, T. M., Ziebart, M. K., Jah, M. K., and Cefola, P. J., "Refining Space Object Radiation Pressure Modeling with Bidirectional Reflectance Distribution Functions," Proceedings of the AAS/AIAA Spaceflight Mechanics Conference, Kauai, HI, February 2013

[2] Vallado, D. A., Fundamentals of Astrodynamics and Applications, McGraw-Hill, New York, NY, 3rd ed., 2007, pp. 707-717.

[3] Ashikhmin, M., and Shirley, P., "An Anisotropic Phong BRDF Model," Journal of Graphics Tools, Vol. 5, No. 2, 2000, pp. 25-32.

[4] Schlick, C., "An Inexpensive BRDF Model for Physically-Based Rendering," Computer Graphics Forum, Vol. 13, No. 3, 1994, pp. 233-246.

[5] Ziebart, M., "Generalized Analytical Solar Radiation Pressure Modeling Algorithm for Spacecraft of Complex Shape," Journal of Spacecraft and Rockets, Vol. 41, No. 5, Sept-Oct 2004, pp. 840-848.